China Geology 8 (2025) 740−753

China Geology

Journal homepage: http://chinageology.cgs.cn
https://www.sciencedirect.com/journal/china-geology

Characteristics of strike-slip fault-related fractures and their controls on reservoir in Halahatang area, northern Tarim Basin

Xiao-xu Liu[a], Guang-hui Wu[a, b], Li-xin Chen[c], Bing-shan Ma[a,*], Zhou Su[c], Bo Yang[c], Xia Wang[c], Bin Zhao[c]

[a] *School of Geoscience and Technology, Southwest Petroleum University, Chengdu* 610500, *China*
[b] *Qiangtang Basin Research Institute, Southwest Petroleum University, Chengdu* 610500, *China*
[c] *PetroChina Tarim Oilfield Company, Korla* 841000, *China*

ARTICLE INFO

Article history:
Received 6 August 2023
Received in revised form 24 March 2024
Accepted 7 June 2024
Available online 22 November 2024

Keywords:
Petroleum system
Strike-slip fault system
Fracture parameters
Fracturing stage
Ordovician
Carbonate rock
Fault damage zone
Fracture-cave reservoir
Oil-gas exploration engineering
Halahatang area
Tarim Basin

ABSTRACT

The strike-slip fault system in the central Tarim Craton controls a complex petroleum system with estimated reserves exceeding 1×10^9 t, the fault-related fractures are important for hydrocarbon accumulation. In this paper, the basic parameters such as density and width of fractures are counted and classified, and the effects of fractures on reservoirs are analyzed. The results show that: (1) Structural fractures and stylolite were widely developed in Halahatang area and experienced at least three stages of activity based on the infilling materials and crosscutting relationship. (2) Fracture density, width, aperture, and dip angle vary in different wells, but the relationship between the above parameters and the distance to the fault core indicates the fracture differences in the fault damage zone and further provides a method to divide the inner units in the fault damage zone. In addition, oil and gas wells with high production mainly concentrate in the inner unit. (3) The infilling materials and degree of fractures vary. Fractures formed in the early stage are more filled and less open, while the fractures formed in the late stage are relatively less filled and more open. (4) Fractures improve porosity to a certain extent but greatly increase permeability, especially in the inner zone of fault damage zone with large quantity, multiple inclinations, less filling and large width. These features contribute to the formation of a higher-quality reservoir, further improving oil and gas production. This paper provides a quantitative characterization method for the study of strike-slip fault-related fracture-caved reservoirs, and points out that fault damage zone, especially the inner zone of the fault damage zone, is the potential goal for oil and gas exploration.

1. Introduction

Faulting and fracturing in the upper crust play a pivotal role in shaping fault-related hydraulic properties and subsequent geological deformations (Faulkner DR et al., 2010; Bense VF et al., 2013). The fractures generated through tectonism, along with their associated features are crucial to the formation and transformation of carbonate rock fracture karst reservoir. The fractures transform the reservoir by enhancing fluid activity, thus improving the reservoir permeability of carbonate rock reservoir (Graham WBR et al., 2006; Pöppelreiter M et al., 2005; Larsen B et al., 2010; Su J et al., 2010), further controlling the hydrocarbon accumulation and enrichment. While predecessors have examined the types, stages, causes, and relationships between fractures and karst reservoir (Gao JX et al., 2012; Wu GH et al., 2019), there remains a dearth of comprehensive anatomical analysis and statistical evaluation.

The Tarim Basin stands as the largest petroliferous basin in China (Fig. 1; Jia CZ, 1997; Tang LJ et al., 2014; Wu GH et al., 2016; Deng S et al., 2019). In the central craton of Tarim Basin, extensive intercratonic strike-slip fault systems govern a complex petroleum system boasting estimated reserves exceeding 1 billion tons (Lu XB et al., 2017; Jiao FZ, 2018; Wu GH et al., 2020). In the deep and tight Ordovician limestone reservoir, fracture-related reservoirs along the strike-slip fault zones is the main targets for exploration. In the Halahatang area, the distribution and architecture of the reservoir are intricately shaped by strike-slip faults and differential karst from north to south. In its initial phases,

First author: *E-mail address*: 2974591892@qq.com (Xiao-xu Liu).

* Corresponding author: *E-mail address*: mabingshan09@163.com (Bing-shan Ma).

Literary editor: Xi-jie Chen
doi:10.31035/cg2023085
2096-5192/© 2025 China Geology Editorial Office.

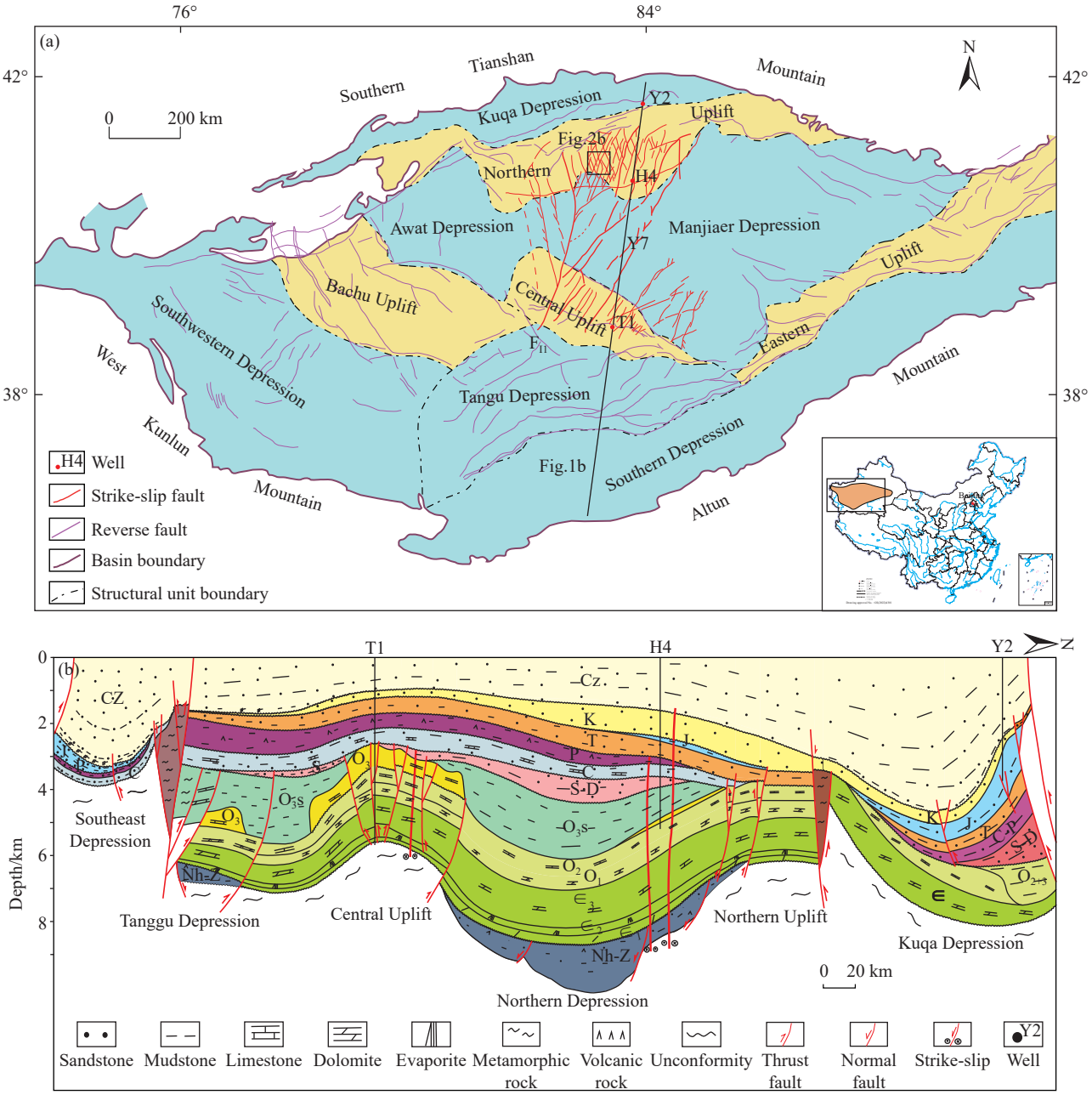

Fig. 1. a–Tectonic division in the Tarim Basin (the right corner icon shows the location in China, China basemap after China National Bureau of Surveying and Mapping Geographical Information) (after Wu GH et al., 2016); b–SN-striking geological profile across the Tarim Basin (modified from Wu GH et al., 2016, 2020) (profile location is shown in Fig. 1a).

karst was regarded as a pivotal factor controlling reservoir, resulting in ambiguous distribution patterns of efficient and inefficient wells. However, there is a lack of statistical data on the impact of fractures on reservoir.

In this paper, we have calculated the pertinent parameters of fractures in over 20 wells to present the characteristics of fractures in the Halahatang area, analyzing the relationship between fractures and fault damage zones, and discussing the influence of fractures on reservoir.

2. Geological setting

The Tarim Basin is the largest petroliferous basin in China covering 560×10^3 km^2 (Fig. 1a; Jia CZ, 1997; Xie HZ et al., 2023). It consists of the Cenozoic foreland basin and Palaeozoic-Mesozoic intracratonic basin, following multi-phase tectonic movements (Fig. 1b; Jia CZ, 1997; Tang LJ et al., 2014; Wu GH et al., 2016). The Tarim Basin developed thick Late Neoproterozoic-Quaternary sedimentary sequences covering Archean-Early Neoproterozoic crystalline basement (Fig. 1b), which recorded the supercontinent assembly and breakup in late Neoproterozoic, and the opening and closure of the Tethys in Palaeo-Mesozoic, and the Indo-Asian collision in Cenozoic (Jia CZ, 1997; Wu GH et al., 2016).

The study area, encompassing approximately 8000 km^2, is located on the southern slope of the Northern Uplift of Tarim Basin (Fig. 1). The Phanerozoic strata consist of Cambrian-Ordovician carbonates, Silurian-Cretaceous siliciclastic

successions with multiple unconformities and a Cenozoic sequence representing rapid subsidence (Fig. 1b; Jia CZ, 1997; Wu GH et al., 2018).

The Cambrian-Ordovician carbonates form a generally uniform succession deposited in the inner platform (Li Q et al., 2010; Wu GH et al., 2016; Zhang YQ., 2020) with a carbonate thickness of 2500–3000 m. The Cambrian-Lower Ordovician rocks primarily consist of dolomites, transitioning progressively into Middle-Upper Ordovician limestones. Notably, multiple tectonic events and unconformities, spanning from the Late Ordovician to the Cenozoic (Fig. 1b), have contributed to the diverse distribution of the marine-terrestrial siliciclastic strata (Jia CZ, 1997; Wu GH et al., 2016). In the Halahatang area, the Cambrian-Ordovician carbonate exhibits a south-dipping slope with a buried depth ranging from 6000 m to 7500 m.

During the Sinian to Quaternary, the basin underwent a complex tectonic evolution (Zhang GY et al., 2007), involving multiple complicated extension-compression processes (Wei GQ and Jia CZ, 1998). This evolution included distinct stages such as the Sinian strong extension-compression stage, the Cambrian-Ordovician weak extension-strong compression stage, the Silurian-Cretaceous intracratonic oscillation and up-down transition stage, and the subsequent Cenozoic weak extension-strong compression stage. The tectonic movements in the Middle-Late Caledonian period, Hercynian period, Indosinian, Yanshanian, Himalayan period, and other major periods induced different styles of structural deformation in different periods and parts of the Tarim Basin. A conjugate NE and NW trending strike-slip fault system have been identified in the Cambrian-Ordovician carbonates (Figs. 2 and 3; Sun D et al., 2015; Wu GH et al., 2018). These faults, with maximum lengths reaching up to 70 km within the Cambrian-Ordovician carbonates (Figs. 2 and 3; Wu GH et al., 2018), exhibit dihedral angles ranging from 26° to 51° in the Ordovician carbonates (Wu GH et al., 2018), indicative of a nearly N-S maximum principal stress orientation.

3. Data and method

Cores from over 20 wells, which penetrated the Ordovician carbonates along fault damage zones in the Halahatang area of northern Tarim Basin, were available for study. These enable core and thin section data to be used in describing the fractures. Fractures were characterized by parameters such as fracture proportion, density, filling material, degree, effective fracture width, and others. The fracture parameters in cores of more than 20 wells were calculated. Additionally, an analysis was performed to explore the relationship between these parameters and their distance to the fault. On this basis, the division of fault damage zone and fractures' influence on the reservoir were analyzed.

4. Parameter statistics of structural fractures

4.1. Fracture types

The typical "X" type strike-slip fault system was well developed in the Halahatang area (Fig. 2b), accompanied by numerous small-scale strike-slip faults. Despite the challenges in identifying these fractures at the seismic scale, the characteristics of fractures observed in cores and thin sections

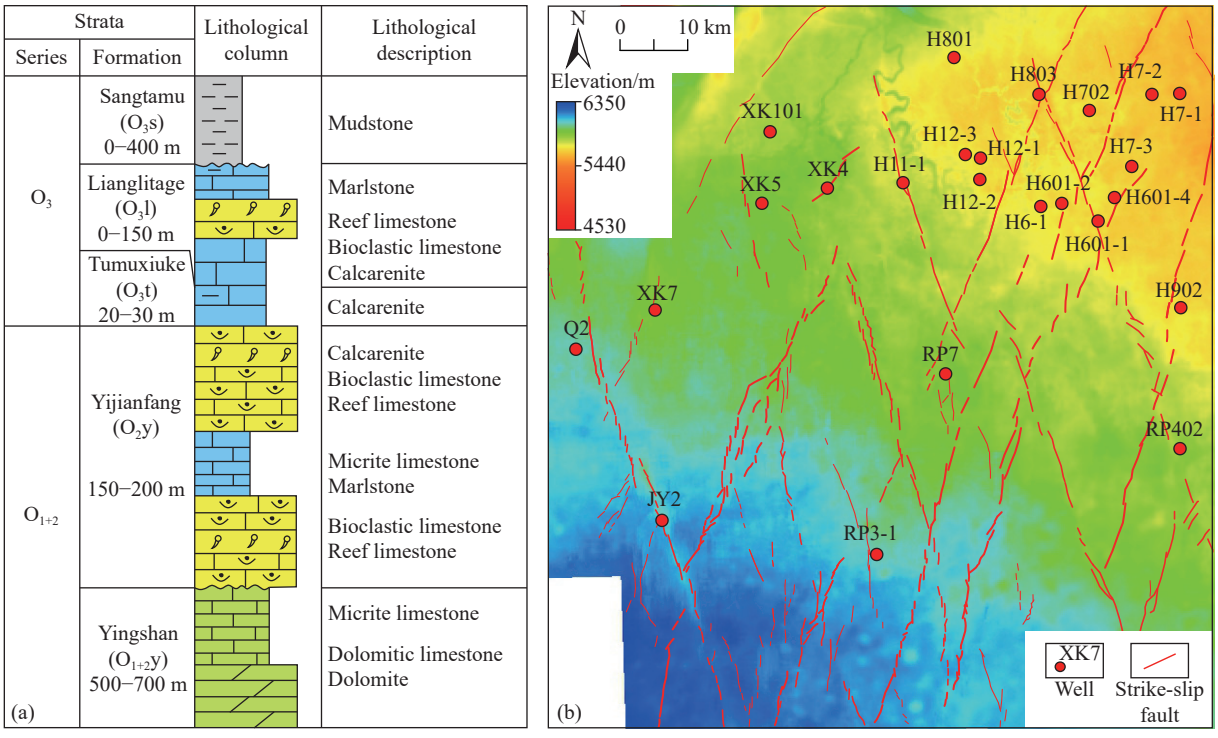

Fig. 2. Stratigraphic column of the Ordovician carbonate (a) (modified from Wu GH et al., 2016; Wan XG et al., 2016) and the strike-slip fault system of the bottom surface of the Tumuxiuke Formation (b).

from the Ordovician reservoir in the Halahatang area are highly pronounced (Figs. 3, 4). These fractures are believed to be derivatives resulting from multi-stage fault activity and represent a significant response to the strike-slip fault activity.

Multiple classification schemes for fractures exist in the core of the Halahatang area, each based on distinct principles (Gao JX et al., 2012). According to fracture orientation, they can be divided into vertical, oblique, and horizontal fractures, as well as stylolite, such as horizontal and vertical stylolites. The horizontal and low-angle micro-fractures have different characteristics with uneven distribution. The vertical micro-fractures, which are formed late and cut early-stage fractures and vugs, are commonly developed in all wells and exert a significant influence on the seepage of the reservoirs.

Almost all fractures can be classified into three types based on their mechanisms: Structural fractures, diagenetic fractures, and polygenetic fractures. Structural fractures result from tectonic stress caused by regional tectonic movements, such as faulting and folding. These fractures in the Halahatang area were induced by widespread strike-slip faults and multi-type karst corrosion fractures.

Several different multi-stage fracture types in the Ordovician carbonates, including en echelon, conjugate, sub-vertical, and tail-spraying fractures (Fig. 3). These fractures exhibit diverse filling materials, including mud, calcite, or bitumen impregnations (Fig. 3).

Some semi-infilled and open fractures also can be observed. Fractures filled with calcite display a simple geometry, stable strike orientation, large spacing, and wide extension range, and mostly appear in the middle and lower part of each well. The mud-infilled fractures are irregular and interlaced like a network, which cut the early suture. The phenomenon that calcite enlarges the filling in the later period could be observed. Some mud-filled fractures were found to be contaminated with iron. In addition, fractures are not uniformly filled with just one type of material.

The pressure solution fractures (stylolites) in the Halahatang area are also extremely developed, including horizontal pressure solution fractures with varying widths and degrees of filling, as well as structural pressure solution fractures mixed with structures (Fig. 4). The distribution of diagenetic fractures is constrained by bedding, occurring parallel to the bedding surface, and fewer of them penetrated layers with irregular shapes. Structural corrosion fractures display irregular patterns with partial corrosion remnants, a result of structural dissolution. These fractures typically develop in the same direction as pressure dissolution fractures and are filled with materials such as mud and calcite.

4.2. Fracture formation stages

The formation order of fracture can be determined based on the crosscutting relationship between fractures (Fig. 5). Based on observations from thin sections, the crosscutting relationships reveal three distinct cycles of fracture activities, with later fractures exhibiting a higher proportion of unfilled fractures. The first-stage fractures (f1, f denotes the fractures throughout the paper) are nearly filled by narrow fine calcite and are cut across by the second-stage fracture (f2) (Fig. 5b). The second-stage fractures are commonly wider than the first-stage fractures and larger apertures are observed in thin

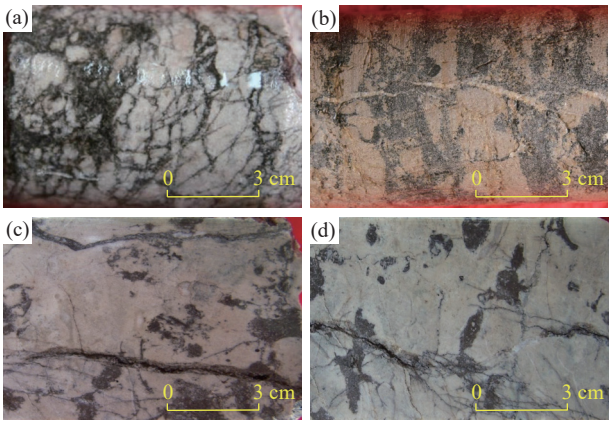

Fig. 3. Photographs of structural fractures from the cores of the Ordovician carbonate strata in the Halahatang area. a–conjugate fracture networks, b–en echelon tension fractures with calcite filling, c–sub-vertical half-infilling fracture, d–fracture expansion, filling, and splaying micro-fractures at the tip.

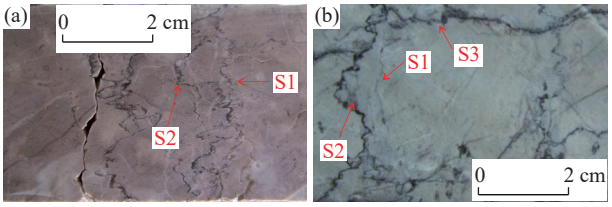

Fig. 4. Photographs of stylolites from core of the Ordovician strata in Halahatang area. a–sub-parallel stylolites in tight limestone; b–the crosscutting relationship shows multiple sequences: Early low-amplitude stylolite (S1), enlarged late high-amplitude stylolite (S2), tectonic stylolite (S3) with late dissolution and calcite cements.

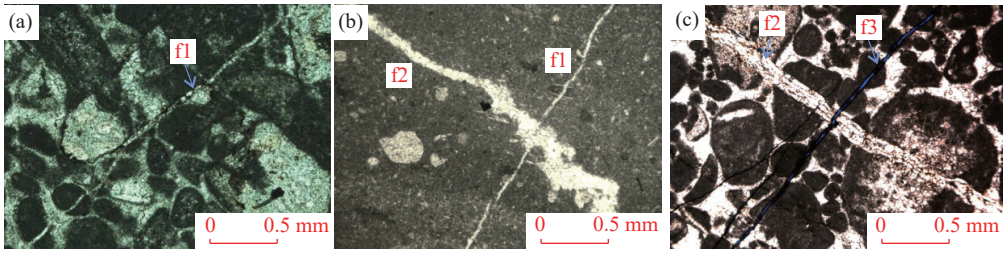

Fig. 5. Photographs of structural fractures from thin sections of the Ordovician carbonate strata in the Halahatang area. a–an early fracture was full-filled with calcite; b–a wider enlarged fracture (f2) crosscut a narrow early fracture (f1), c–an open fracture crosscut a wider enlarged fracture.

sections (Figs. 5a, b). In contrast, most of the late-stage fractures (f3) are open and have limited infilling (Fig. 5c).

Under the microscope, there are three phases of stylolite fractures (Fig. 4): The first is the irregular and wavy structural corrosion line. The local corrosion could be observed. In addition, the fractures are filled with mud, calcite, etc. The second is pressure-dissolved fractures, which are generally developed. Most early-stage fractures are toothed and microwave-like, while most late-stage fractures are peaking and serrated. Dissolution and tracking fractures are observable in this phase. The third is the commonly developed micro-fractures, which cut early-stage calcite-filled fractures, or pressure solution fissures. These fractures typically display relatively straight surfaces, with the majority remaining unfilled.

4.3. Parameter statistical result

4.3.1. Fracture density

Statistical analysis of fracture density is usually carried out based on the number of fractures per unit core length in petroleum production and application. However, due to the incomplete casting of thin sections in core samples and the frequent absence or breakage of core samples in sections with well-developed fractures, this paper adopts a unit of strips/blocks to study fracture density.

In Fig. 6, fracture density generally ranges from 5 to 7.5, reaching a peak of 8.57 in well JY2, but only 0.4 and 1.5 in well H601–2 and H601–4. The limited number of thin sections in some wells contributes to the constrained countable fractures, potentially explaining the lower density in those wells. The variation in fracture density along the longitudinal direction is considerable. In some wells, the fractures are not developed, while in some wells, the dense fractures occur, and the difference in fracture density is more than 10 times, which underscores the pronounced heterogeneity in fracture distribution. On a regional scale, the density of fractures is higher in the north and south, whereas the density of fractures in local wells in the middle is lower. Wells situated farther from the strike-slip fault, such as H601–2 and XK5 (Figs. 2b, 6a, b), demonstrate a notably low fracture density.

4.3.2. Fracture filling materials

According to the filling materials of fractures, the fractures can be classified into four types: (1) Lime-mud filling, which mainly occurs in horizontal stylolites and some structural fractures; (2) Calcite filling, divided into sparry calcite and micrite calcite, with at least three stages of calcite filling. This type may exhibit visible dissolution edges or be associated with minerals; (3) Organic matter filling, there is more asphaltic filling in carbonate fractures in the Halahatang area, which is more associated with calcite and mud. In addition, there are pyrite and siliceous fillings, but they are mostly associated with other fillings. In the Halahatang area, fractures in Ordovician carbonate rocks are predominantly filled with calcite. In contrast, the Lower Ordovician weathering crust is filled with mud (Fig. 6c). From north to south, the amount of well infilled by calcite gradually increases.

Based on the observation and analysis of the cores and thin sections, fractures are predominantly filled with calcite or mud, with filling rates ranging from 50% to 80%. The unfilled fractures are primarily micro-fractures. Although most of the fractures are filled, there are still oil, bitumen impregnation and solution vugs, indicating that a substantial portion of fractures continues to contribute to the reservoir.

According to the degree of fracture filling, it can be divided into three types of fractures: the first is the unfilled fractures. It mostly consists of micro-fractures; the second is the semi-filled fractures with diverse filling materials and different filling degrees. These fractures are mostly infilled by calcium, mud and other components of different degrees of filling, and local pore residual or dissolution holes can be observed along the fractures; third is the fully infilled fractures, with more early-stage infilled calcite (Fig. 6d). In the Halahatang area, full-filling fractures are more commonly developed, and calcite is usually observed as full filling material in structural fractures, while mud filling is mainly observed in pressure solution fractures in non-structural fractures.

4.3.3. Fracture opening property and effective width

According to the open-seal property of fractures, fractures can also be categorized into effective open fractures and ineffective closed fractures. Unfilled fractures and semi-filled fractures generally possess gaps conducive to fluid flow, qualifying them as open fractures. In contrast, many ineffective closed fractures do not facilitate fluid transport except during active structural periods. The aperture of fractures is relative and changes under different conditions. The partial filling effect of fractures, where secondary minerals act as natural supports, can prevent closure, potentially rendering fractures effective for fluid transport in deep underground environments. Even the fully filled fractures, some parts can form local extension stress to induce the fractures to open and become favorable transport channels under certain temperature and pressure conditions. Generally speaking, the fractures formed in the early stage are characterized by more filling and lower aperture, while the fractures formed in the late stage are characterized by relatively less filling and higher aperture. The degree of fracture filling increases with greater burial depth, with carbonate cement filling significantly increasing, possibly due to enhanced temperature and pressure effects. The aperture of fractures displays substantial variability, and the density of open fractures typically ranges from 0.3–3 pieces/m, with proportions varying between 20% and 70% (Fig. 7). The aperture of fractures varies among different wells and well sections. The ratio of opening fracture of well H801 is about 80%–90%, while the ratio of opening fracture of well H601–2, H11–1and XK5 is below 20%. It may also be caused by a lack of thin sections.

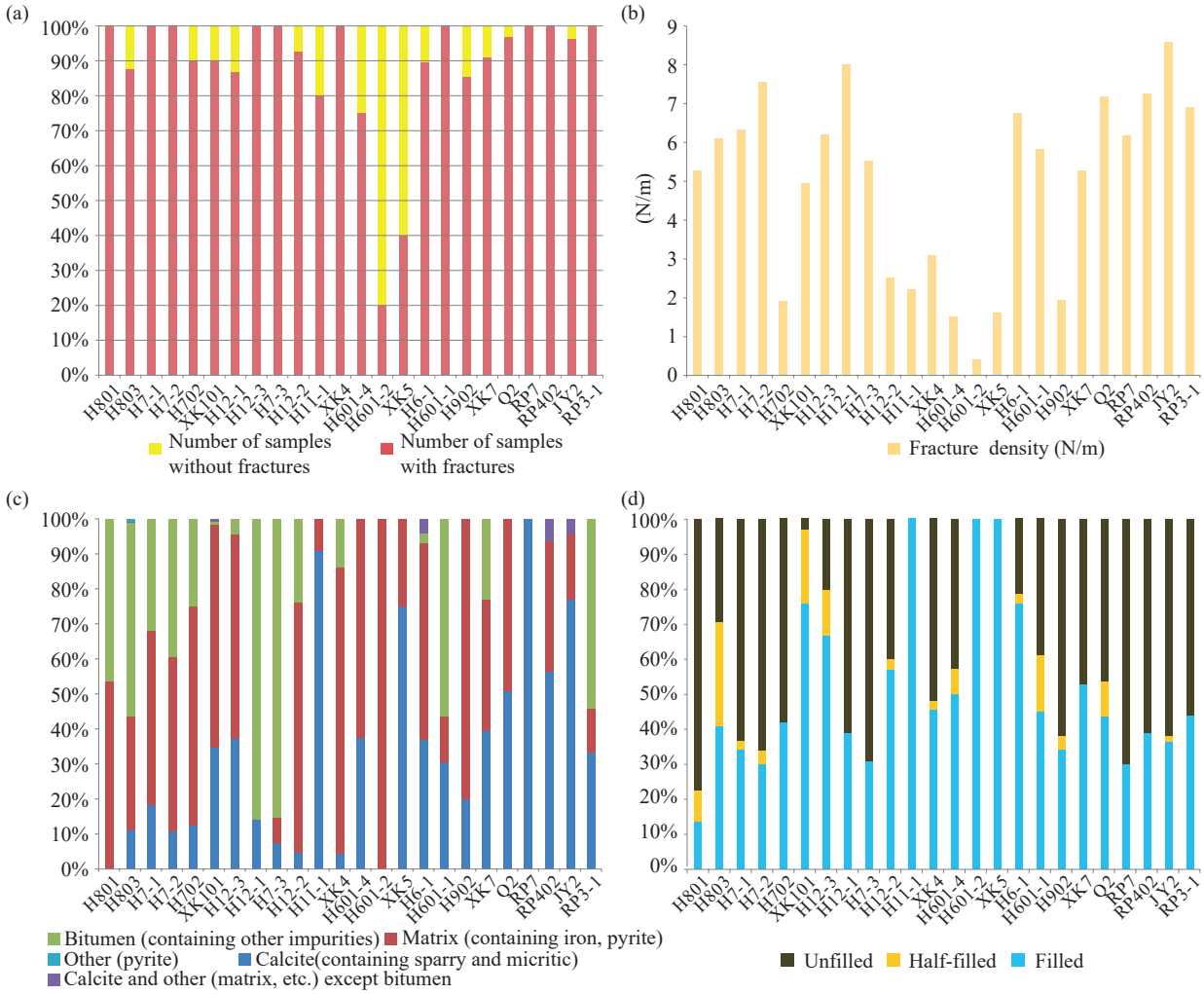

Fig. 6. a–Fracture distribution of different wells in the Halahatang area; b–average fractures density of drilling wells in the Halahatang area; c–types of fracture infilling materials in Halahatang area; d–ratio of fracture filling in Halahatang area.

The effective width of a fracture is defined as the distance between the two inner surfaces of the fracture. The usual fracture width refers to the average fracture width. The effective fracture width refers to the real flow characteristics of the fracture, according to the relationship between fluid flow and hydraulic opening. This parameter is crucial for calculating fracture porosity and permeability, offering a direct assessment of the impact of fractures on exploitation. In this paper, the data of effective fracture width obtained from the thin sections are analyzed statistically. It was observed that the effective width of fractures in this area generally falls below 0.5 mm, with a concentration in the range of 0.01–0.05 mm (Fig. 8). Notably, H902 stands out with 32 fractures having effective widths of 0.01 mm. However, the effective widths of 5 wells including JY2, RP3–1, RP7 and RP402 are smaller, with the main effective widths being 0.001–0.01mm.

4.4. Fracture-related reservoir physical properties

4.4.1. Reservoir distribution and characteristics

The reservoirs of Halahatang Oilfield are mostly distributed along the strike-slip faults and exhibit significant differences in seismic attribute maps from the surrounding rock. Therefore, the fracture-cave reservoir along the strike-slip fault can be predicted and described.

In the southern part of the study area, controlled by strike-slip faults, the associated fault damage zone formed with a limited scale. The fracture-cave reservoir developed near the fault core are mostly adjacent to the strike-slip fault damage zone, forming the linear reservoir. The strike-slip fault not only controls the fracture network but also controls the occurrence and development of epigenetic karstification and buried dissolution.

In the central part, the major faults and the secondary faults form an irregular fracture zone with varying width, which is superimposed by the later karst water system transformation to form fracture-cave reservoirs with a large and dispersed boundary. This type of reservoir is controlled by both the strike-slip fault and the interlayer karstification. The interlayer karst fracture-cave reservoir is more developed along the strike-slip fault damage zone, and it is also developed outside the fault damage zone.

In the northern part, the Ordovician carbonate rocks were uplifted and eroded on a large scale, and experienced multiple karstification, forming a weathering crust karst reservoir. The

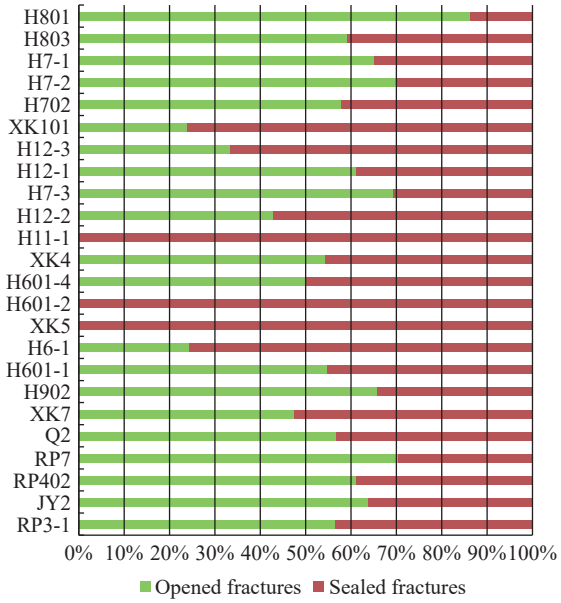

Fig. 7. Ratio of open and sealed fractures calculated from cores in Halahatang area.

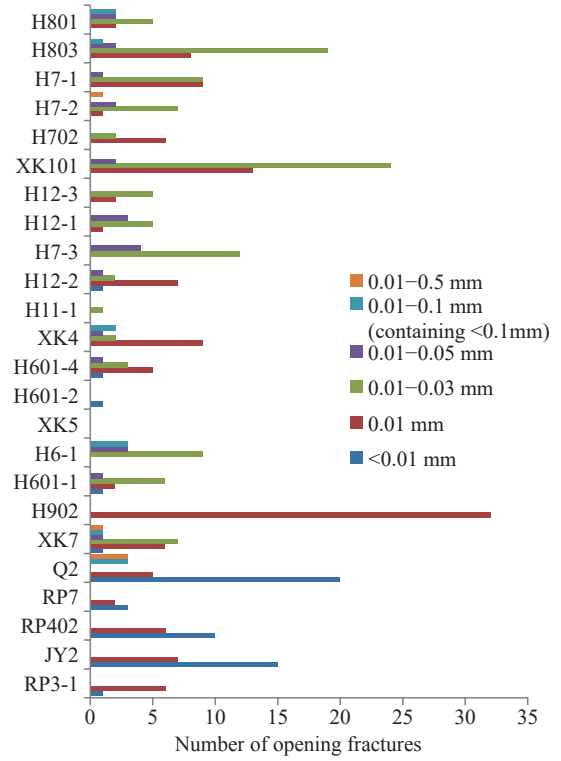

Fig. 8. Opening fracture width calculated from cores in Halahatang area.

fracture network is enlarged by dissolution to form the fracture-cave reservoir. This type of reservoir exceeds the fault damage zone and is distributed in a blocky style.

4.4.2. Porosity and permeability

Fractured reservoir is commonly developed in tight carbonate reservoir, where fractures serve as the primary reservoir and interconnected channels. The original rock in such reservoir typically exhibits poor physical properties, with underdeveloped primary and secondary pores. According to the reservoir distribution map (Fig. 9), wells that are counted herein are distributed near strike-slip faults, which induce a large amount of fractures. These fractures are widely observed in cores and contribute to increased porosity and permeability in the reservoir to some extent. However, the pore-permeability correlation diagram for this area (Fig. 10) reveals that the positive correlation is not highly evident. Notably, in some low-porosity core samples, the permeability increases significantly, indicating the presence of fractures and micro-fractures. In addition, the permeability in the sample with fracture exhibits a substantial increase, spanning several orders of magnitude, in contrast to samples without fracture.

Most fracture porosity in fractured reservoirs is distributed in a wide range of 0.5%–10%. The fracture rate is about 0.05%–0.3% calculated from the core of Ordovician carbonate strata, and the higher fracture rate is about 0.1%–0.5%. The fracture rate from thin sections is generally 0.05%–0.2%, and a few can reach 1%–3%. Fracture porosity derived from well logging interpretation exhibits a wider variation, typically ranging from 0.001% to 0.8%, with a magnitude order of about 0.1%. Overall, fracture porosity in the Halahatang area is relatively low, falling within the range of 0.01–0.1%.

The width of fractures varies from 0.01 cm to 10 cm, but the broader fractures are typically filled with calcite or mud, and the aperture of effective fractures is generally on the order of 0.1 mm. The width of effective fractures is mostly in the range of 0.005–0.05 mm as observed in the thin sections, the width of individual fractures can reach 0.3–1.2 mm, and the width of micro-fractures is on the order of 0.01 mm. Although the width of microfractures is usually small, potentially less than the diameter of a pore, the permeability of the matrix can be significantly enhanced in the direction parallel to the fracture orientation. At depths of 4000 m to 7000 m, the fracture aperture is less open, but it could not close completely and could not hinder the migration of oil and gas.

5. Discussion

5.1. Implication for division of fault damage zone

The Halahatang area is characterized by a prominent conjugate strike-slip fault system, and the fault damage zone plays a critical role in controlling the reservoir, hydrocarbon accumulation and oil-gas production. The fault damage zone in carbonate rocks exhibits a complex structure and heterogeneity, typically consisting of the inner zone with an intense deformation zone and the outer zone dominated by peripheral fractures. Generally speaking, the degree of fracture development in the fault damage zone decreases with the increase in distance from the fault core (Mitchell TM and Faulkner DR, 2009; Savage HM and Brodsky EE, 2011; Faulkner DR et al., 2011; Torabi A and Berg SS, 2011; Choi JH et al., 2016), therefore the boundaries of the inner architecture of the fault damage zone could be divided by the abrupt change of fracture density.

However, the fracture distribution varies greatly, and there

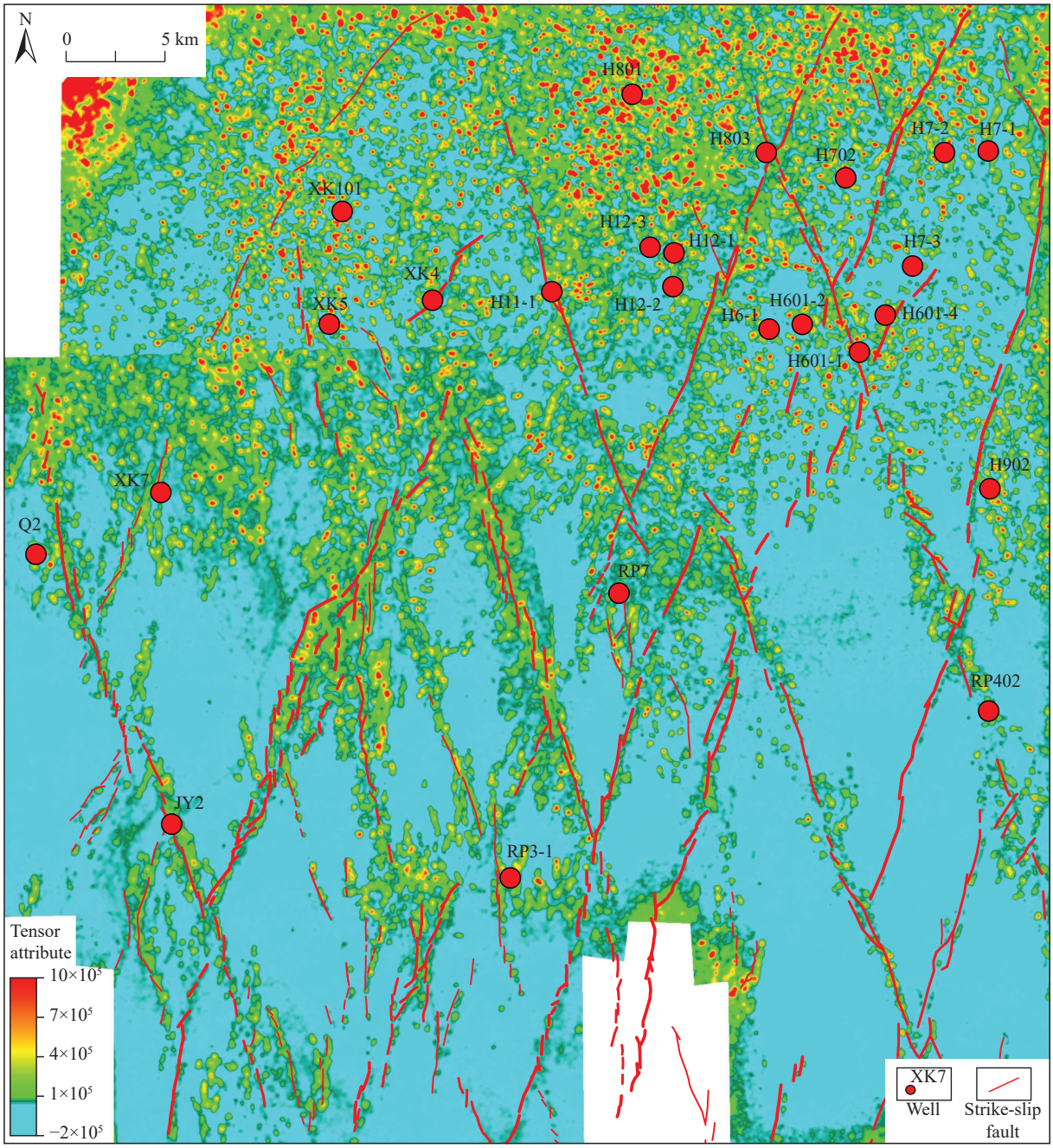

Fig. 9. Tensor attribute illustrating fractured-cave reservoir superimposed by strike-slip faults in Halahatang area.

may be a gradual distribution along the boundary of the fault damage zone, making it challenging to determine the specific location of the fault damage zone (Choi JH et al., 2016; Wu GH et al., 2019). In addition, obtaining underground data in sedimentary basin is limited, and it is difficult to identify fractures, which are difficult to determine on the conventional fracture distribution map. Therefore, accurately identifying the strike-slip fault damage zone is crucial. Based on the law of fracture variation, Choi JH et al. (2016) proposed a method of fracture accumulation frequency, which addresses the challenge of accurately determining the boundary of the fault damage zone due to the gradual change in fracture density (frequency) from the fault damage zone to the surrounding rock. When the application of this method is in the outcrop area, the width of the fault damage zone can be more accurately determined, and the fracture accumulation frequency can be used to determine whether it is located in the fault damage zone (Choi JH et al., 2016). Combined with outcrop observation, this method has a good effect on the external boundary of the outcrop fault damage zone, but due to the strong heterogeneity of fracture distribution, whether the borehole encounters the fault damage zone cannot be solely determined according to the frequency of core fractures in a well. Comprehensively analysis of statistical parameters from many wells could be a suitable method to identify the inner boundary of fault damage zone.

In the Halahatang area, the fracture distribution characteristics of Ordovician carbonate rocks are obviously

different from those of stable surrounding rock areas. The statistical analysis of core and logging shows that fracture parameters are controlled by the fault damage zone. The inner zone and outer zone of the fault damage zone can be roughly distinguished according to the characteristics of fracture distribution, such as fracture dip angle, inclination and width (Fig. 11). The fracture dip angle in the inner zone of the fault damage zone changes greatly, but the fracture dip angle increases gradually towards the outer zone and surrounding rock zone (Fig. 11a). The inclination of fracture (Fig. 11c) undergoes a similar alteration at the corresponding position compared to Figure 14a. Fracture width tends to increase with the increase of fracture dip angle (Fig. 11b). And diagram of fracture width vs. distance to fault also illustrates the obvious division boundary between inner and outer zones.

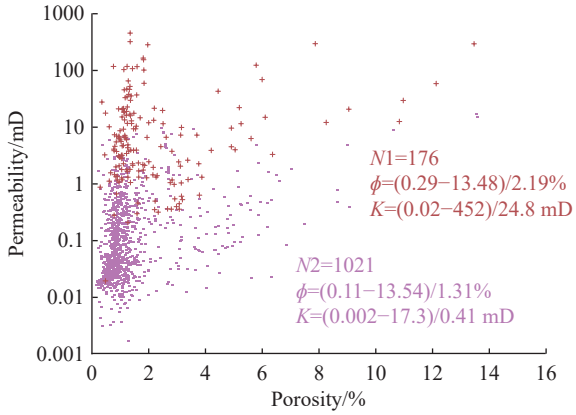

Fig. 10. Correlation diagram of porosity and permeability of Ordovician carbonate rocks (N1 is the sample with fracture, N2 is the sample without fracture).

Change of cumulative fracture frequency curves, as observed in both logging and thin sections, also suggests the division boundary between the inner zone and outer zone of fault damage zone (Fig. 12). In addition, the inner and outer zones of the fault damage zone also can be roughly distinguished according to the characteristics of fracture width (Fig. 13). The fracture width explained by logging is less than 0.1 mm, indicating a low degree of opening for underground fractures. The aperture of fractures is relatively small, and small fractures are relatively developed, accounting for a proportion generally greater than 75%, contributing to the overall fracture development. The filling degree of fractures in the inner zone is low, mainly consisting of late unfilled to semi-filled small fractures. However, only a small number of small and medium-sized fractures are mainly developed in the surrounding rock area, and the filling degree is high. To sum up, the inner zone of the fault damage zone is characterized by large fractures, elevated aperture, substantial width and low filling, which controls the distribution of high-quality reservoirs, and further high oil-gas production (Fig. 14a). Notably, high-yield wells are predominantly situated within an approximate range of about 1800 m from the fault (Fig. 14a). The cumulative oil production per unit pressure drop curve also suggests the interior boundaries of fault damage zone (Fig.14b).

It is worth noting that determining the approximate boundary of the fault damage zone is generally based on the observed fracture development patterns, but it lacks a scientific research plan. By integrating information on the structure of fractured zones and drilling data, such as fracture density and cumulative density, it becomes feasible to identify

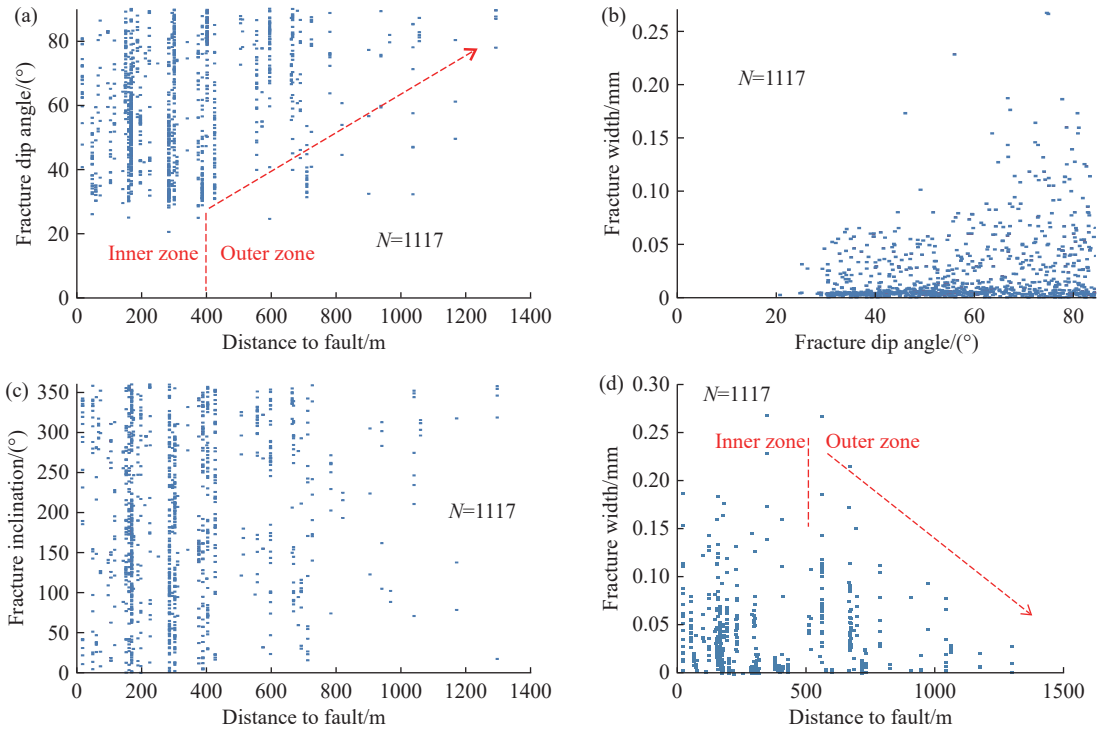

Fig. 11. Statistical diagram of fracture dip tendency of Ordovician core (a, b, c) and statistics of fracture width (d) in Ordovician carbonate cores in Halahatang area.

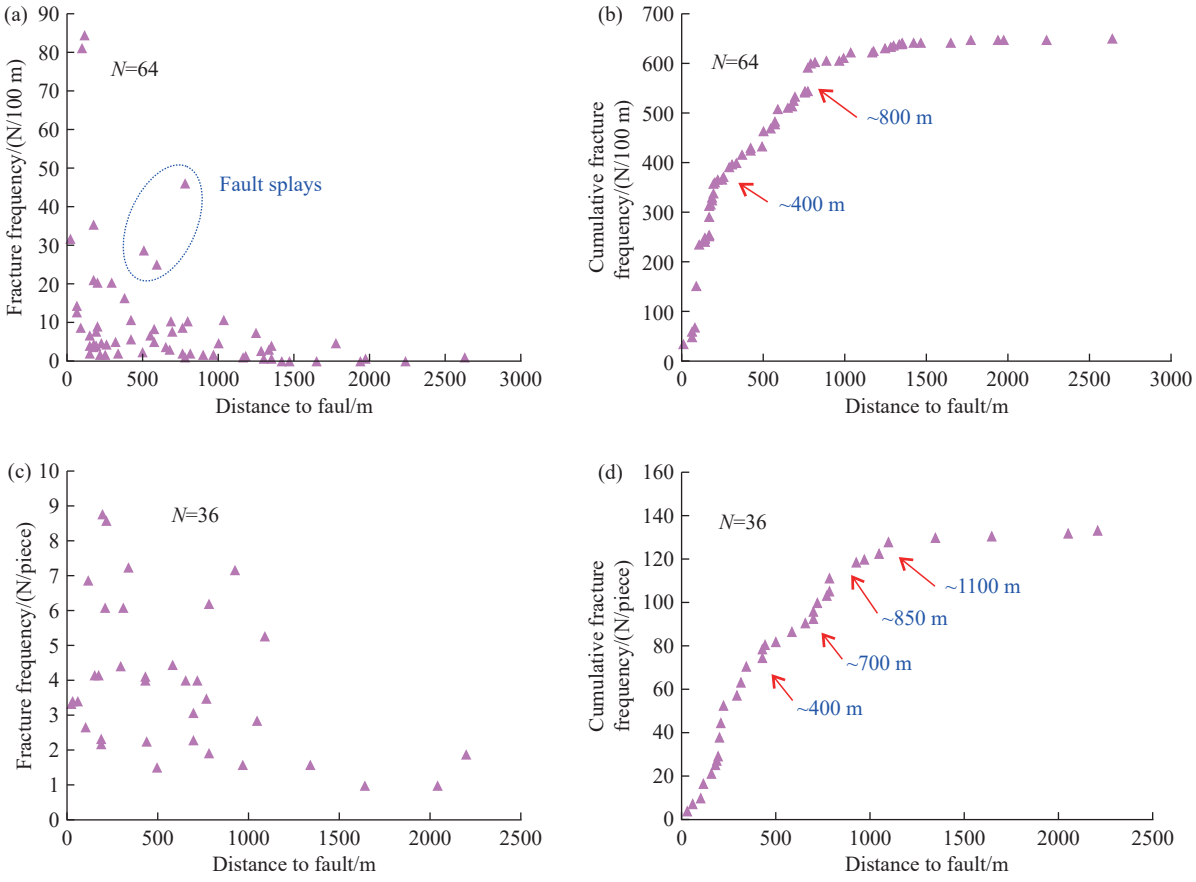

Fig. 12. Frequency of fractures vs. distance to fault (a, b data from logging; c, d data from the thin sections) (modified from Wu GH et al., 2019).

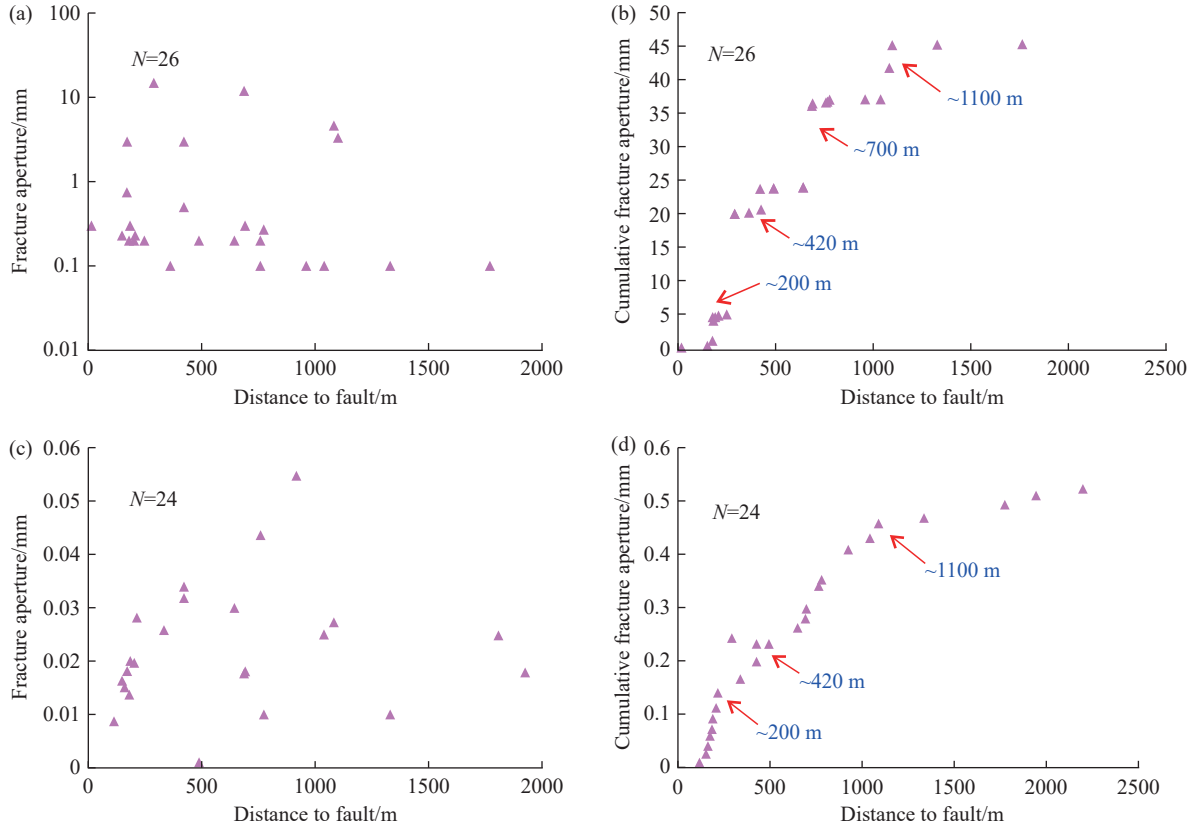

Fig. 13. Aperture of fracture vs. distance to fault (a, b from the core; c, d from the thin section data) in the Halahatang area (modified from Wu GH et al., 2019).

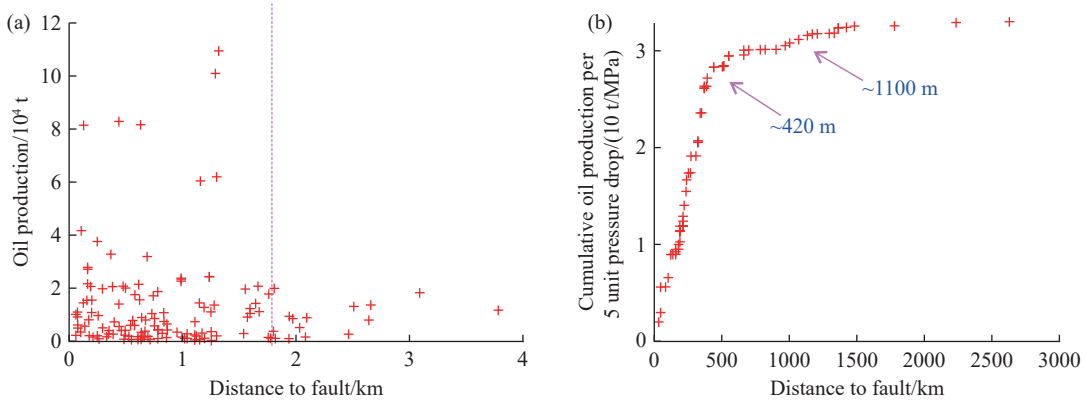

Fig. 14. Crude oil production vs. distance to fault (a, b) in Halahatang area (modified from Wu GH et al., 2019).

underground fault damage zones (Choi JH et al., 2016; Wu GH et al., 2019). In the Halahatang area, the density and aperture of fractures decrease with distance to fault decrease (Figs. 12a, c; 13a, c). The cumulative density curves and cumulative aperture curves therefore suggest the boundaries of the fault damage zone. Based on the data related to fracture distribution, it is believed that there are several boundaries of fault damage zones in the Halahatang area (Figs. 12b, d; 13b, d). In addition, in the sedimentary basins controlled by strike-slip faults, the statistics of oil and gas parameters can also indicate the boundaries of fault damage zones to a certain extent (Figs. 14a, b).

5.2. Controls on physical properties and styles of reservoir

5.2.1. Effective influence of fractures on porosity and permeability

The Tarim Basin has experienced multi-stage tectonic movements, and carbonate rocks have developed multi-stage and multi-type fracture systems. In heterogeneous and low permeability carbonate reservoirs, the development degree and opening of fault damage zones play an important role in improving the porosity and permeability of the reservoir.

Based on the analysis of cores and thin sections, the porosity of fracture is low, and the reservoir space of Ordovician carbonate rocks in the Tarim Basin is predominantly characterized by secondary dissolution caves, which mostly experience the process of early dissolution and filling, and then dissolution again. Small faults and fractures are commonly associated with these dissolution holes, indicating that the late-stage dissolution may be related to fractures as channels. Although the porosity of fractures is low, the presence of dissolved pores, intergranular pores, and intra-granular pores along fractures is widespread in most thin sections. Corrosion fractures, or structural fractures after corrosion, are frequently observed in cores, displaying varying widths, with some reaching up to 0.2mm to 5mm (Figs. 12a, b). In the northern weathering crust area, the dissolution fractures are mainly at low angles, and the dissolution usually occurs along the structural fractures or stylolite. The percentage of fractures and related dissolved pores observed in thin sections can reach 0.5%–3%, contributing significantly to the effective reservoir space and constituting 10% to 30% of the total reservoir porosity. Fractures are not only an important part of tight carbonate reservoirs but also play an important role in the development of dissolved caves.

Although the fracture porosity is generally low and the aperture is small, fractures exhibit high connectivity, and their width exceeds the pore radius of the matrix pore by a considerable margin. This characteristic has a more significant impact on permeability than on porosity, which is supported by statistical results of single well porosity and permeability (Fig. 10). Even a slight increase in fracture porosity can lead to a substantial change in permeability, particularly in the direction parallel to the fractures. The permeability values obtained by the carbonate rock oil test can be regarded as the overall response of a large range of reservoirs. The values are generally low, and most of them are comparable to the matrix permeability, indicating that the connectivity between fractures is limited and the reservoir is not completely connected. The primary medium facilitating connection between oil and gas reservoirs is predominantly the matrix pores. However, in the inner zone of the fault damage zone, especially after superposing karst channels or weathering crust, faults/fractures play an important role in forming high-quality reservoirs, and the proportion of high-yield wells closer to faults increases.

5.2.2. Formation of fracture-related reservoir styles

Recent research indicates that fault-controlled reservoir is distributed along the strike-slip fault zone, with the northern Tarim Craton being a prominent example (Jiao FZ et al., 2018; Yun L et al., 2021; Wang Q et al., 2021; Tian J et al., 2021). In the Halahatang area, the interaction of weathering crust in the buried hill area and karst channels in the coverage area, coupled with the fault damage zone controlled the reservoir styles in the northern and southern areas.

In the northern Halahatang area, the buried hill area is also mostly affected by fault reconstruction, forming a reservoir enrichment area along the fault damage zone (Sun XM et al., 2016). At the same time, the strike-slip fault zone also underwent a complex reconstruction of weathering crust karst and buried karst. The main oil and gas storage space is mainly

composed of large-scale dissolution fracture cave systems with strong heterogeneity of reservoir. Reservoir spaces in this region manifest in four main types, namely cave-type, pore-type, fracture-type, and fracture-pore-type. Drilling data reveals that the most common reservoir encountered in this area is the fracture-type reservoir, followed by fracture-pore-type and fracture-type. The most productive reservoir is a cave-type reservoir, followed by a fracture-pore-type reservoir. In addition, the distribution of cave-type reservoirs is predominantly aligned with the strike-slip fault, and concentrates within a certain range (about 800 m) of fault, which basically belongs to the fault damage zone.

Fractured reservoir in the area primarily consist of fractures along with a limited number of solution pores distributed along layers. Effectively fractured reservoir is characterized by multiple groups of fractures connecting with each other or fractures connecting with the solution pores and caves reservoir spaces. The fracture occurrence varies greatly in this area, including high-angle, low-angle, and even horizontal fractures, with a predominant presence of middle- and high-angle fractures. Both core and well-logging data indicate that the fractures enhancing storage space in this area are predominantly high-angle fractures with long extensions.

In the southern coverage area, the fracture-cave type reservoir primarily comprises secondary dissolution pores, where fractures enhance permeability and reservoir, facilitating connection between the pores and fractures. It is mainly developed in the Upper Ordovician Lianglitage Formation reef beach reservoir in platform margin and the Middle Ordovician Yijianfang Formation granulated limestone reservoir within open platform facies, showing quasi-stratified distribution.

5.3. Impact on fracture-related reservoir exploration in fault damage zone

In the northern Tarim cratonic basin, a large number of high-quality carbonate fracture-cave reservoir with multi-stage karst superposition are still developed at a depth of more than 7000 m. The seismic response characteristics are mainly manifested by strong beaded reflection, and the fracture-cave reservoir are highly heterogeneous and distributed along fault damage zones (Sun XM et al., 2016; Lu XB et al., 2017). In recent years, with the beneficial development of ultra-deep fault-controlled karst reservoir in marine carbonate rocks such as Halahatang, Fuman, Shunbei, Shunnan and Tazhong in the Tarim Basin, it has been proved that strike-slip faults have an obvious controlling effect on ultra-deep carbonate reservoir in the Ordovician in the Tarim craton basin (Jiao FZ, 2018; Jiang TW et al., 2021; Yun L et al., 2021; Wang Q et al., 2021; Tian J et al., 2021; Ma YS et al., 2022).

The matrix permeability of Ordovician dense carbonate rock in the Tarim Basin is generally lower than 0.5×10^{-3} um^2, even in areas with well-developed reef bodies, where permeability generally remains below 1×10^{-3} μm². Despite the extensive presence of oil in the reef beach, production is typically modest. Currently, reef beach reservoirs generally undergo large-scale acid fracturing, which may increase production capacity by more than five times, forming industrial oil and gas flows. Through the process transformation measures of large-scale acid fracturing, low-production oil, and gas flow wells may obtain high-production industrial oil and gas flow, indicating that through reservoir transformation, the connectivity of fracture and cave systems can be greatly improved, effectively improving oil and gas production.

The Lower Paleozoic carbonate rocks in the Tarim Basin are generally low permeability fractured reservoirs, and fractures have a great effect on porosity and permeability, but they are not completely connected to form a whole high permeability reservoir, resulting in strong heterogeneity of the reservoir. In some areas, there are moderately developed fracture reservoirs in the Ordovician carbonate rocks where fracture connectivity is robust, significantly enhancing reservoir permeability. Additionally, there are instances of fractured reservoirs characterized by poor matrix physical properties, dominance of fractures, relatively small scale, high initial production, but rapid subsequent decline.

Under similar fracture characteristics, differences in oil and gas production can vary significantly, sometimes by several times or even tens of times, due to variations in fracture connectivity resulting from spatial arrangements. A fractured reservoir system with good connectivity can maintain high and stable oil and gas production, but poor connectivity not only has low production, but also difficult to stabilize production. In summary, while fractures contribute to the effective reservoir space and permeability in the carbonate rocks of the Tarim Basin, the distribution, scale, and connectivity of fractures are critical factors influencing the production of oil and gas from carbonate reservoirs. The inner zone of the fault damage zone is proven to develop fractures characterized by large quantity, multiple inclinations, less filling and large width. These features contribute to the formation of a higher-quality reservoir. This research points out the exploration and exploitation direction for tight carbonate rocks with faults.

6. Conclusions

(i) The fracture density exhibits significant heterogeneity across different wells in the Halahatang area. Some wells show limited development in fracture density, while others exhibit dense fractures, resulting in differences exceeding 10 times and highlighting the strong heterogeneity in fracture distribution. Structural fractures and stylolite were widespread observed in both core and thin sections in the Halahatang area and experienced at least three stages of activity based on the infilling materials and crosscutting relationship.

(ii) Fracture density, width, aperture, and dip angle vary in different wells, but the relationship between the above parameters and the distance to the fault core indicates the fracture differences in the fault damage zone. Several

boundaries within the internal zone, such as approximately 400 m, were identified through various diagrams depicting the relationship between different parameters and the distance to the fault. The relationship between oil and gas production and the distance to the fault core can also, to some extent, reflect the boundaries of the inner units within the fault damage zones.

(iii) The infilling materials and degree of fractures exhibit variation. Fractures formed in the early stage tend to be more filled and less open, whereas fractures formed in the late stage are relatively less filled and more open.

(iv) The low porosity of fractures is the typical feature in the Halahatang area, but there are generally dissolution pores, intergranular pores and intra-granular pores along the fractures, and the fractures increase the porosity to some extent. The permeability of the fractured interval is much higher than that of the general reservoir and surrounding rock, which proves that most reservoirs have poor connectivity. Fractures play a crucial role in enhancing permeability, thereby influencing oil and gas production.

(v) The fault damage zone together with karstification influences the reservoir styles and controls the distribution of high-quality reservoir and high-yield wells in a certain range from the strike-slip fault, where the inner zone of fault damage zone mostly develops.

CRediT authorship contribution statement

Bing-shan Ma and Guang-hui Wu conceived of the presented idea. Li-xin Chen and Guang-hui Wu supervised the findings of this work. Xiao-xu Liu and Bing-shan Ma contributed to the interpretation of the results. Xiao-xu Liu, Bing-shan Ma, Zhou Su, Bo Yang, Bin Zhao wrote the manuscript in consultation. All authors discussed the results and contributed to the final manuscript.

Declaration of competing interest

The authors declare no conflicts of interest.

Acknowledgement

We thanked two anonymous reviewers, together with editor Profs. Zi-guo Hao, for their constructive comments focusing us on improving the manuscript. PetroChina Tarim Oilfield Company was thanked for permission for publication. This study was jointly supported by the Natural Science Foundation of China-Youth Foundation (42402163), Natural Science Foundation of Sichuan Province of China (2024NSFSC0814), and Science and Technology Cooperation Project of the CNPC-SWPU Innovation Alliance (2020CX010101). Hao Tang and Wei-zhen Tian were thanked for their kind help during the preparation of the manuscript.

References

Bense VF, Gleeson T, Loveless SE, Bour O, Scibek J. 2013. Fault zone hydrogeology. Earth-Science Reviews, 127, 171–192. doi: 10.1016/j.earscirev.2013.09.008.

Graham WBR, Girbacea R, Mesonjesi A, Aydin A. 2006. Evolution of fracture and fault-controlled fluid pathways in carbonates of the Albanides fold-thrust belt. AAPG Bulletin, 90(8), 1227–1249. doi: 10.1306/03280604014.

Choi JH, Edwards P, Ko K, Kim YS. 2016. Definition and classification of fault damage zones: A review and a new methodological approach. Earth-Science Reviews, 152, 70–87. doi: 10.1016/j.earscirev.2015.11.006.

Deng S, Li HL, Zhang ZP, Zhang JB, Yang X. 2019. Structural characterization of intracratonic strike-slip faults in the central Tarim Basin. AAPG Bulletin, 103(1), 109–137. doi: 10.1306/06071817354.

Faulkner DR, Jackson CAL, Lunn RJ, Schlische RW, Shipton ZK, Wibberley CAJ, Withjack MO. 2010. A review of recent developments concerning the structure, mechanics and fluid flow properties of fault zones. Journal of Structural Geology, 32(11), 1557–1575. doi: 10.1016/j.jsg.2010.06.009.

Faulkner DR, Mitchell TM, Jensen E, Cembrano J. 2011. Scaling of fault damage zones with displacement and the implications for fault growth processes. Journal of Geophysical Research-Solid Earth, 116(B5), B05403. doi: 10.1029/2010jb007788.

Gao JX, Tang JW, Zhang XF, Tao XW, Yang YK, Chen ZY, Song XM, Liu B. 2012. Types and episodes of fractures in carbonate cores from the Ordovician Yijianfang Formation in the Halahatang area, northern Tarim Basin. Acta Petrolei Sinica, 33(1), 64–73 (in Chinese with English abstract). doi: 10.7623/syxb201201008.

Jia CZ. 1997. Tectonic characteristics and petroleum, Tarim basin, China: Beijing: Geological Publishing House, 29–261 (in Chinese).

Jiao FZ. 2018. Significance and prospect of ultra-deep carbonate fault-karst reservoirs in Shunbei area, Tarim Basin. Oil and Gas Geology, 39(2), 207–216 (in Chinese with English abstract). doi: 10.11743/ogg20180201.

Jiang TW, Chang LJ, Deng XL, Li SY, Wu GH, Wan XG, Guan BZ. 2021. Geological understanding and evaluation technology of fault controlled carbonate reservoir development: A case study of the Tarim Basin. Natural Gas Industry, 41(3), 1–9 (in Chinese with English abstract). doi: 10.3787/j.issn.1000-0976.2021.03.001.

Larsen B, Grunnaleite I, Gudmundsson A. 2010. How fracture systems affect permeability development in shallow-water carbonate rocks: An example from the Gargano Peninsula, Italy. Journal of Structural Geology, 32(9), 1212–1230. doi: 10.1016/j.jsg.2009.05.009.

Li Q, Wu GH, Pang X, Pan W, Luo C, Wang C, Li XS, Zhou B. 2010. Hydrocarbon Accumulation Conditions of Ordovician Carbonate in Tarim Basin. Acta Geologica Sinica-English Edition, 84(5), 1180–1194. doi: 10.1111/j.1755-6724.2010.00289.x.

Lu XB, Wang Y, Tian F, Li XH, Yang DB, Li T, Lv YP, He XM. 2017. New insights into the carbonate karstic fault system and reservoir formation in the Southern Tahe area of the Tarim Basin. Marine and Petroleum Geology, 86, 587–605. doi: 10.1016/j.marpetgeo.2017.06.023.

Ma YS, Cai XY, Yun L, Li ZJ, Li HL, Deng S, Zhao PR. 2022. Practice and theoretical and technical progress in exploration and development of Shunbei ultra-deep carbonate oil and gas field, Tarim Basin, NW China. Petroleum Exploration and Development, 49 (1), 1–20. doi: 10.11698/ S1876-3804(22)60001-6.

Pöppelreiter M, Balzarini MA, De Sousa P, Engel S, Galarraga M, Hansen B, Marquez X, Morell J, Nelson R, Rodriguez F. 2005. Structural control on sweet-spot distribution in a carbonate reservoir: Concepts and 3-D models (Cogollo Group, Lower Cretaceous, Venezuela). AAPG Bulletin, 89(12), 1651–1676. doi: 10.1306/08080504126.

Mitchell TM, Faulkner DR. 2009. The nature and origin of off-fault damage surrounding strike-slip fault zones with a wide range of

displacements: a field study from the Atacama fault system, northern Chile. Journal of Structural Geology, 31(8), 802–816. doi: 10.1016/j.jsg.2009.05.002.

Savage HM, Brodsky EE. 2011. Collateral damage: evolution with displacement of fracture distribution and secondary fault strands in fault damage zones. Journal of Geophysical Research-Solid Earth, 116(B3), B03405. doi: 10.1029/2010jb007665.

Su J, Zhang SC, Yang HJ, Zhu GY, Chen JP, Zhang B. 2010. Control of fault system to formation of effective carbonate reservoir and the rules of petroleum accumulation. Acta Petrolei Sinica, 31(2), 196–203(in Chinese with English abstract). doi: 10.1016/S1876-3804(11)60008-6.

Sun D, Yang LS, Wang HY, Zheng DM, Sun QH, Li GH, Dai DD, Fang QF. 2015. Strike-slip fault system in Halahatang area of Tarim Basin and its control on reservoirs of Ordovician marine carbonate rock. Natural Gas Geoscience, 26(S1), 80–87 (in Chinese with English abstract). doi: 10.11764/j.issn.1672-1926.2015.S1.0080.

Sun XM, Wei HX, Zhai W, Shi GY, Liang YH, Mo RW, Han MX, Yi JZ, Zhang XG. 2016. Fluid inclusion geochemistry and Ar–Ar geochronology of the Cenozoic Bangbu orogenic gold deposit, southern Tibet, China. Ore Geology Reviews, 74, 196–210. doi: 10.1016/j.oregeorev.2015.11.021.

Tang LJ, Huang TZ, Qiu HJ, Wan GM, Li M, Yang Y, Xie DQ, Chen G. 2014. Fault systems and their mechanisms of the formation and distribution of the Tarim Basin, NW China. Journal of Earth Science, 25(1), 169–182. doi: 10.1007/s12583-014-0410-1.

Tian J, Yang HJ, Zhu YF, Deng XL, Xie Z, Zhang YT, Li SY, Cai Q, Zhang YQ, Huang LM. 2021. Geological conditions for hydrocarbon accumulation and key technologies for exploration and development in Fuman oilfield, Tarim Basin. Acta Petrolei Sinica, 42(8), 971–985(in Chinese with English abstract). doi: 10.7623/syxb202108001.

Torabi A, Berg SS. 2011. Scaling of fault attributes: a review. Marine and Petroleum Geology, 28(8), 1444–1460. doi: 10.1016/j.marpetgeo.2011.04.003.

Wan XG, Wu GH, Xie E, Zhang YT, Gao LH. 2016. Seismic prediction of fault damage zones in carbonates in Halahatang area, Tarim Basin. Oil and Gas Geology, 37(5), 786–791 (in Chinese with English abstract). doi: 10.11743/ogg20160519.

Wang Q, Hao F, Cao Z, Tian JQ, Cong F. 2021. Geochemistry and origin of the ultra-deep Ordovician oils in the Shunbei field, Tarim Basin, China: Implications on alteration and mixing. Marine and Petroleum Geology, 123, 104725. doi: 10.1016/j.marpetgeo.2020.104725.

Wei GQ, Jia CZ. 1998. Structural characteristics and oil & gas of thrust belts in Tarim Basin. Editorial office of Acta Petrolei Sinica, 19(1), 11–17(in Chinese). doi: 10.7623/syxb199801003.

Wu GH, Gao LH, Zhang YT, Ning CZ, Xie E. 2019. Fracture attributes in reservoir-scale carbonate fault damage zones and implications for damage zone width and growth in the deep subsurface. Journal of Structural Geology, 118, 181–193. doi: 10.1016/j.jsg.2018.10.008.

Wu GH, Yang HJ, He S, Cao SJ, Liu X, Jing B. 2016. Effects of structural segmentation and faulting on carbonate reservoir properties: A case study from the Central Uplift of the Tarim Basin, China. Marine and Petroleum Geology, 71, 183–197. doi: 10.1016/j.marpetgeo.2015.12.008.

Wu GH, Yuan YJ, Huang SY, Vandyk TM, Xiao Y, Cai Q, Luo B. 2018. The Dihedral Angle and Intersection Processes of a Conjugate Strike-Slip Fault System in the Tarim Basin, NW China. Acta Geologica Sinica - English Edition, 92(1), 74–88. doi: 10.1111/1755-6724.13495.

Wu GH, Zhao KZ, Qu HZ, Scarselli N, Zhang YT, Han JF, Xu YF. 2020. Permeability distribution and scaling in multi-stages carbonate damage zones: Insight from strike-slip fault zones in the Tarim Basin, NW China. Marine and Petroleum Geology, 114, 104208. doi: 10.1016/j.marpetgeo.2019.104208.

Xie HZ, Zhu XK, Wang X, He Y, Shen WB. 2023. Petrological and geochemical characteristics of mafic rocks from the Neoproterozoic Sugetbrak Formation in the northwestern Tarim Block, China. China Geology, 6(1), 85–99. doi: 10.31035/cg2021067.

Yun L. 2021. Controlling effect of NE strike-slip fault system on reservoir development and hydrocarbon accumulation in the eastern Shunbei area and its geological significance, Tarim Basin. China Petroleum Exploration, 26(3), 41–52. doi: 10.3969/j.issn.1672-7703.2021.03.004.

Yun L. 2021. Hydrocarbon Accumulation of Ultra-Deep Ordovician Fault-Karst Reservoirs in Shunbei Area. Xinjiang. Petroleum Geology, 42(2), 136–142 (in Chinese). doi: 10.7657/XJPG20210202.

Zhang GY, Zhao WZ, Wang HJ, Li HH, Liu L. 2007. Multicycle tectonic evolution and composite petroleum systems in the Tarim Basin. Oil and Gas Geology, 28(5), 653–663 (in Chinese with English abstract). doi: 10.3321/j.issn:0253-9985.2007.05.017.

Zhang YQ, Guo ZH, Chen DZ. 2020. Porosity distribution in cyclic dolomites of the Lower Qiulitag Group (Upper Cambrian) in northwestern Tarim Basin, China. China Geology, 3(3), 425–444. doi: 10.31035/cg2020026.